INTERNATIONAL JOURNAL OF ADVANCE RESEARCH AND DEVELOPMENT

(Volume3, Issue2)

Available online at www.ijarnd.com

Modified Form of Reynolds Equation for Porous Cosine-Form Convex Curved Plates with Couplestress Effects

Syed Arishiya Naseem Fatima[1], Trimbak Biradar[2,] and Hanumagowda B. N[4]

[1] *Department of Mathematics, K.C.T College of Engineering, Gulbarga, Karnataka*
[2] *Department of Mathematics, Sharnbasveshwar College of Science, Gulbarga, Karnataka*
[3]*Department of Mathematics, Reva University, Bangalore, Karnataka*

ABSTRACT

This paper presents the theoretical study of couplestress effect on the squeeze film lubrication of cosine form of convex curved plates in which the upper plate has rough structure and the lower plate is with porosity in the presence of an externally applied magnetic field.The gap between the plates is filled with the non-Newtonian conducting lubricant of the film thickness H ***which consists of nominal smooth and rough part. The modified Reynold's equation is derived using Christensen's stochastic theory for rough surfaces. Expressions for dimensionless pressure distribution, load carrying capacity and squeeze film time are derived. The solution of the modified Reynold's equation is obtained and for various physical parameters the results are discussed in terms of squeeze film characteristics of the bearings and graphs are plotted for the results. It is seen that for couplestresses in the presence of transverse magnetic field surface roughness effects are more prominent as compared to non-conducting Newtonian fluid (NCNF) in case of cosine form of convexly curved plates. Tabulated values show, for increased values of couplestress parameter, magnetic and roughness parameter load capacity and squeeze film time increases in transverse roughness case and these quantities decrease in case of longitudinal roughness and also decrease in load carrying capacity and response time is seen in case of permeability compared to the impermeable case.***

Keywords: *Convex Curved Plates, Cosine Function, Magnetic Field, Porous Medium, Surface Roughness, Couplestress Effect.*

1. INTRODUCTION

In flow analysis, Magneto-hydrodynamics (MHD) characteristic are important for industrial applications and in engineering in recent years. Bearings with MHD and conducting fluids possess high thermal and electrical-conductivity features over the conventional bearings. In presence of transverse magnetic field, the squeeze film lubrication for different configuration of bearings has been discussed by several authors [1-9]. The MHD bearings with conducting fluids possess numerous advantages over the conventional bearings.

Christensen [10] studied stochastic model for hydrodynamic lubrication of rough surfaces. Bujurke and Kudenatti [11] studied the combined effects of MHD and surface roughness and found that under the action of transverse magnetic field roughness effect is considerable on the squeeze film characteristics of the bearings. On the basis of Darcy's model porous squeeze film bearings are analyzed, where in the porous matrix the fluid flow obeys Darcy's law and a viscous fluid between them is displaced in the case of two approaching surfaces. The time of approach of the surfaces considerably reduces if one (or) both of the approaching surfaces are porous because from the sides of the porous matrix the lubricant gets squeezed out and also moves into the pores. Therefore self-lubricating characteristics and design simplicity proved porous bearings useful. Thus many authors [12-15] studied the combined effect of roughness and porousness on the bearing.

Stokes [16] presented the theory of couplestress fluid which is a generalization of viscous fluid theory with couplestresses and body couples. Couplestress fluids are the result of the assumption that, across a surface, the interaction of one part of the body on another is equivalent to a force and momentum distribution. It consists of rigid randomly oriented particles suspended in a viscous medium such as electro-rheological fluids and synthetic fluids. Many studies have investigated the effect of surface roughness and couplestress on the squeeze film lubrication in the presence of transverse magnetic field [17].

The effect of surface roughness on MHD conducting couplestress squeeze-film characteristics between the cosine form convex curved plates with porosity has not been studied so far. Hence, in this paper, an attempt has been made to obtain the modified form of Reynolds equation to study the combined effect of surface roughness and porosity effects with conducting couple stresses on the MHD squeeze-film characteristics between the cosine forms of convex curved plates. Expressions for the MHD squeeze-film pressure, load carrying capacity and the time-height relation are obtained.

2. MATHEMATICAL FORMULATION OF THE PROBLEM

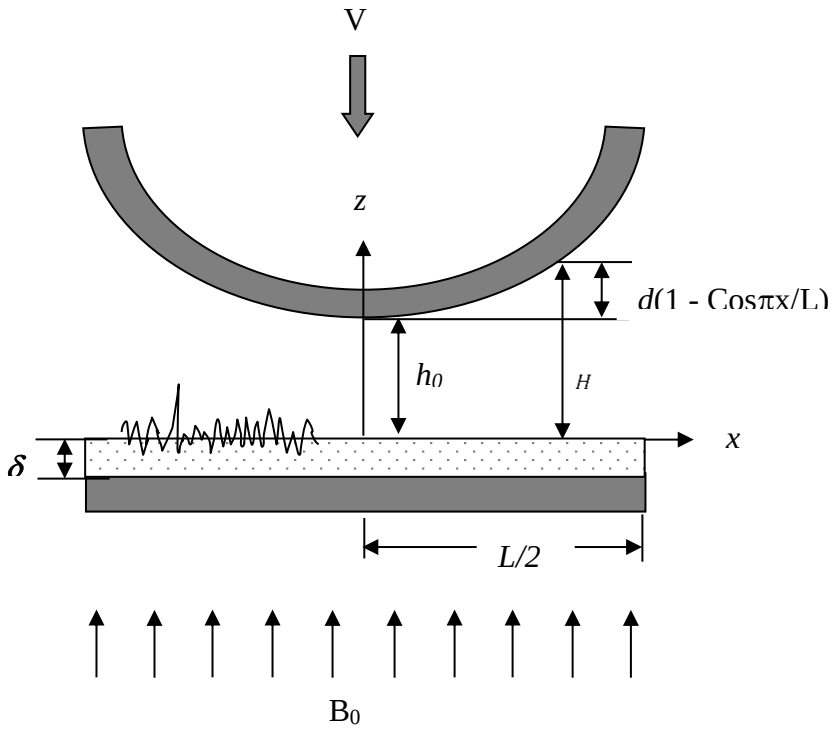

Figure 1: Porous and Rough Cosine form Convex Curved Plates with Transverse Magnetic Field

Considering the squeeze flow between rough and porous cosine form convex curved plates, with squeezing velocity $V = \partial H / \partial t$ approaching each other. Between the thickness of the plate of the film is given by H . For the squeeze film H can be given by the cosine function form $H = h_0 + d\left\{1 - \cos\left(\frac{\pi}{L}x\right)\right\}$ in which h_0 is the minimum thickness of the film, d is cosine function's amplitude and L represents the length of the plates. The thickness of the film is equal to h_0 at the mid position: $x = 0$ and the sum of minimum film thickness and the amplitude $h_0 + d$ gives film thickness at the edge: $x = L/2$. Different sizes of convex curved surfaces can be obtained by changing the amplitude's value for the cosine function for a fixed length L using the above equation.

Supposing that the fluid film is thin hence the body forces and the body couples are unimportant but Lorent'z body force is considered which represents the third term of equation (1). Under the supposition of thin film's hydrodynamic lubrication theory and Stokes theory for couple stresses, the equation of continuity and the MHD governing equations of motion in Cartesian coordinate are

$$\mu \frac{\partial^2 u}{\partial z^2} - \eta \frac{\partial^4 u}{\partial z^4} - \sigma B_0^2 u = \frac{\partial p}{\partial x} \tag{1}$$

$$\frac{\partial p}{\partial z} = 0 \tag{2}$$

$$\frac{\partial u}{\partial x} + \frac{\partial w}{\partial z} = 0 \tag{3}$$

Where $M_0 = \frac{M}{h_0}$ and $M_0 = B_0 h_0 (\frac{\sigma}{\mu})^{1/2}$ is the Hartmann number.

p is the film pressure, u and w are the velocities of the fluid in $x-$ and $z-$ direction respectively, μ is the lubricant viscosity, η is material constant responsible for couplestresses, $l^2 = \frac{\eta}{\mu}$ is couplestress parameter, σ being the conductivity of the lubricant.

A uniform transverse magnetic field B_0 is applied to the bearing in the z-direction as shown in the Figure1.

Boundary Conditions are:

i) At the upper surface $z = H$

$u = 0$ (no slip), $\frac{\partial^2 u}{\partial z^2} = 0$ (vanishing of couplestresses), (4)

ii) At the lower surface $z = 0$

$u = 0$ (no slip), (vanishing of couplestresses), $w = w^*$ (5)

Where w^* is the modified Darcy velocity component in the $z-$ direction of the porous area. For porous material modified form of the Darcy law is given by

$$u^* = -\frac{k}{\mu\left(1-\beta+\frac{kM_0^2}{mh_0^2}\right)}\frac{\partial p^*}{\partial x} \quad (6)$$

$$w^* = -\frac{k}{\mu(1-\beta)}\frac{\partial p^*}{\partial z} \quad (7)$$

Where is porous matrix permeability, m porosity and p^* is the porous area pressure? $\beta = (\eta/\mu)/k$, i.e, the ratio of the microscopic size of the additives to the size of the pores. If $\beta \approx 1$ then the pores of the porous area get obstructed by the microscopic additives of the lubricant resulting in reduced Darcy flow through the porous region if β 1 then the additives get into the pores of the porous area easily. From (6) and (7) Newtonian fluid flow is seen in the porous region if. Due to continuity pressure p^* satisfies Laplace equation

$$\frac{\partial^2 p^*}{\partial x^2} + N\frac{\partial^2 p^*}{\partial z^2} = 0 \quad (8)$$

Where $N = \left(1-\beta+\frac{kM_0^2}{mh_0^2}\right)\Big/(1-\beta)$

Integrating above equation once with respect to z from $-\delta$ to 0 and using the Morgan-Cameron approximation according to which, in comparison of fluid film area, porous layer thickness is very small, with the condition $\partial p^*/\partial z = 0$ when $z = -\delta$ and also using, at the porous interface $z = 0$, $p = p^*$ i.e, pressure continuity condition gives $\left(\frac{\partial p^*}{\partial z}\right)_{z=0} = -\frac{\delta(1-\beta)}{D}\frac{\partial^2 p}{\partial x^2}$ (9)

Where $D = \left(1-\beta+\frac{kM_0^2}{mh_0^2}\right)$ and δ is the porous layer thickness.

The solution of equation (1) subject to the boundary conditions eqns. (4) and (5) is given by

$$u = -\frac{h_0^2}{\mu M_0^2}\frac{\partial p}{\partial x}\left\{\frac{1}{(A^2-B^2)}\left(\frac{B^2 Cosh\frac{A(2z-H)}{2l}}{Cosh\frac{AH}{2l}} - \frac{A^2 Cosh\frac{B(2z-H)}{2l}}{Cosh\frac{BH}{2l}}\right)+1\right\} \quad (10)$$

Where $A = \sqrt{\left(\frac{1+\sqrt{1-4l^2M_0^2/h_0^2}}{2}\right)}$ and $B = \sqrt{\left(\frac{1-\sqrt{1-4l^2M_0^2/h_0^2}}{2}\right)}$

Taking u value in the integral form of continuity equation

$$\frac{\partial}{\partial x}\left\{\int_0^H u dz\right\} + w_H - w_0 = 0 \quad (11)$$

Substituting (9) and (10) in (11) gives

$$\frac{\partial}{\partial x}\left\{\frac{h_0^2}{\mu}\frac{\partial p}{\partial x} f(H,l,M_0) + \frac{k\delta}{\mu D}\frac{\partial p}{\partial x}\right\} = -\frac{dH}{dt} \quad (12)$$

Where $f(H,l,M_0) = \frac{1}{M_0^2}\left\{\frac{2l}{A^2-B^2}\left(\frac{B^2}{A}\tanh\frac{AH}{2l} - \frac{A^2}{B}\tanh\frac{BH}{2l}\right)+H\right\}$

In the mathematical way to symbolize surface roughness, film thickness is considered to be made up of two parts

$$H = h(t) + h_s(x,z,\xi)$$

Where h stands for the nominal smooth part of the film thickness, h_s is a quantity that varies randomly and thus describes surface roughness quantified from the nominal level and ξ is an index describing the definite roughness arrangements. Let $f(h_s)$ be the probability density function of the random variable h_s. Taking the stochastic average of (12) with respect to $f(h_s)$ the averaged modified Reynold's type equation is obtained in the form

$$\frac{\partial}{\partial x}\left\{\frac{h_0^2}{\mu}\frac{\partial E(p)}{\partial x} E\left(f(H,l,M_0)\right) + \frac{k\delta}{\mu D}\frac{\partial E(p)}{\partial x}\right\} = -\frac{dE(H)}{dt} \quad (13)$$

$E(*)$ Denotes the expectancy operator defined by $E(*) = \int_{-\infty}^{\infty} (*) f(h_s) dh_s$

Following Christensen [10]. We assume that

$$f(h_s) = \begin{cases} \frac{35}{32c^7}(c^2-h_s^2)^3. & -c < h_s < c \\ 0 & elsewhere \end{cases}$$

Where $\sigma = \frac{c}{3}$ is the standard deviation?

In the context of Christensen stochastic theory for the hydrodynamic lubrication of rough surfaces, two types of one-dimensional surface roughness patterns are considered, namely, longitudinal roughness pattern and transverse roughness pattern.

2.1 Longitudinal Roughness

For the one-dimensional longitudinal roughness pattern, the roughness striations are in the form of long narrow ridges and a valley running in the *x*-direction; in this case, the non- dimensional stochastic film thickness assumes the form

$$H^* = h^* + h_s^*(z,\xi)$$

And the stochastic modified Reynold's equation (13) takes the form

$$\frac{\partial}{\partial x}\left\{\frac{h_0^2}{\mu}\frac{\partial E(p)}{\partial x}E\left(f(H,l,M_0)\right)+\frac{k\delta}{\mu D}\frac{\partial E(p)}{\partial x}\right\}=-\frac{dh}{dt} \tag{14}$$

2.2 Transverse Roughness

For the one-dimensional transverse roughness pattern, the roughness structure has the form of long, narrow ridges and valleys running in the *z*-direction, in this case, the non-dimensional stochastic film thickness assume the form

$$H^* = h^* + h_s^*(x,\xi)$$

And the stochastic modified Reynolds equation (13) takes the form

$$\frac{\partial}{\partial x}\left[\frac{h_0^2}{\mu}\frac{\partial E(p)}{\partial x}\frac{1}{E\left(\frac{1}{f(H,l,M_0)}\right)}+\frac{k\delta}{\mu D}\frac{\partial E(p)}{\partial x}\right]=-\frac{dh}{dt} \tag{15}$$

Equations (14) and (15) together can be written as

$$\frac{\partial}{\partial x}\left[\frac{h_0^2}{\mu}\frac{\partial E(p)}{\partial x}G(f(H,l,M_0))+\frac{k\delta}{\mu D}\frac{\partial E(p)}{\partial x}\right]=-\frac{dh}{dt} \tag{16}$$

Where $G(H,l,M_0)=\begin{cases}E(f(H,l,M_0)) & \text{for longitudinal roughness}\\ \{E(1/(f(H,l,M_0)))\}^{-1} & \text{for transeverse roughness}\end{cases}$ (17)

$$E(f(H,l,M_0))=\frac{35}{32c^7}\int_{-c}^{c} f(H,l,M_0)(c^2-h_s^2)^3\,dh_s \tag{18}$$

$$E\left(\frac{1}{f(H,l,M_0)}\right)=\frac{35}{32c^7}\int_{-c}^{c}\frac{(c^2-h_s^2)^3}{f(H,l,M_0)}\,dh_s \tag{19}$$

Introducing nondimensional quantities: $x^*=\frac{x}{L}, H^*=\frac{H}{h_0}, l^*=\frac{2l}{h_0}, p^*=\frac{E(p)h_0^3}{\mu L^2(dh/dt)}, S=\frac{d}{h_0}$,

$$\psi=\frac{k\delta}{h_0^3}, C=\frac{c}{h_0}, \delta^*=\frac{\delta}{h_0}$$

Equation (16) takes the form

$$\frac{\partial}{\partial x^*}\left\{\frac{\partial p^*}{\partial x^*}G^*(H^*,l^*,M_0)+\frac{\psi}{D^*}\right\}=-1 \tag{20}$$

Where $D^*=1-\beta+\frac{\psi M_0^{\,2}}{m\delta^*}$

$$G^*(H^*,l^*,M_0)=\begin{cases}E(F(H^*,l^*,M_0)) & \text{for longitudinal roughness}\\ E(1/(F(H^*,l^*,M_0)))\}^{-1} & \text{for transeverse roughness}\end{cases} \tag{21}$$

$$F(H^*,l^*,M_0)=\frac{h_0}{M_0^2}\left\{\frac{l^*}{A^{*2}-B^{*2}}\left(\frac{B^{*2}}{A^*}\tanh\frac{A^*H^*}{l^*}-\frac{A^{*2}}{B^*}\tanh\frac{B^*H^*}{l^*}\right)+H^*\right\}$$

Where

$$A^*=\sqrt{\left(\frac{1+\sqrt{1-l^{*2}M_0^2}}{2}\right)},\ B^*=\sqrt{\left(\frac{1-\sqrt{1-l^{*2}M_0^2}}{2}\right)}$$

The pressure conditions are: $p^*=0$ at $x^*=\pm\frac{1}{2}$ and $\frac{dp^*}{dx^*}=0$ at $x^*=0$. (21)

Integrating the above non-dimensional stochastic Reynolds type equation with respect to x^*

And using the above boundary conditions, one has

$$p^*=\int_{x^*}^{1/2}\frac{x^*}{G^*(H^*,l^*,M_0)}dx^* \quad (22)$$

Integrating the film pressure, one can obtain the load-carrying capacity

$$E(W)=b\int_{-L/2}^{L/2}E(p)dx$$

Where b denotes the width of the curved plates. Introducing a non-dimensional form gives

$$W^*=\frac{h_0^3E(W)}{\mu L^3 b\,dH/dt}=\int_{-1/2}^{1/2}p^*dx^*$$

After performing the integration, one can obtain the non-dimensional load capacity

$$W^*=\int_{-1/2}^{1/2}\left\{\int_{x^*}^{1/2}\frac{x^*}{G^*(H^*,l^*,M_0)}dx^*\right\}dx^* \quad (23)$$

Introducing non-dimensional time as:

$$T^*=\frac{E(W)h_0^2t}{\mu L^3 b}$$

The elapsed time required for the upper curved plate to approach the lower plate is given by

$$T^*=\int_{h_0^*}^{1}\left[\int_{-1/2}^{1/2}\left\{\int_{x^*}^{1/2}\frac{x^*}{G^*(H^*,l^*,M_0)}dx^*\right\}dx^*\right]dh_0^* \quad (24)$$

Where, $H^*=h_0^*+\delta\{1-\cos(\pi x^*)\}$

Film pressure (22), load capacity (23) and elapsed time (24) can be evaluated using the method of numerical integration.

3. RESULTS AND DISCUSSIONS

Based on Stoke's microcontinuum theory and Christensen's stochastic approach this paper examines the influence of couplestress and surface roughness on the squeeze film characteristic of cosine form of convexly curved plates. Couplestress effects are taken into account because of the presence of additives present in the lubricant and using christensen's theory for rough surfaces stochastic Reynold's equation is derived. For couplestress fluids, a new material constant η is introduced due to substructures contained in the fluid. These substructures molecular length is given by $l=\left(\eta/\mu\right)^{1/2}$ whose value varies in different lubricants. Couplestress

parameter $l^* = \left(2l/h_0\right)$ characterizes couplestress effect on the squeeze film system's performance. Since on the characteristic molecular length of the additives, l^* value depends, therefore l^* can be presented by the characteristic of the fluid interaction with the geometry of the plates. As $l^* \to 0$ the problem reduces to Newtonian lubricant case. On the squeeze film characteristics, the influence of couplestress and roughness are significant for large l^* and roughness parameter C respectively. For low l^* and C values couple stress and roughness effects are slight.

3.1 Squeeze Film Pressure

Figures 2, 3, 4 illustrates the dimensionless pressure P^* as a function of horizontal coordinate x^* at different values of C, M_0 and l^*. Increase in squeeze film pressure is observed in case of transverse roughness because of the ridges in transverse direction in the roughness structure which resists fluid flow thus no fluid escapes, resulting in increased squeeze film pressure as compared to longitudinal roughness case which has ridges in longitudinal direction because of these, no resistance in fluid flow is seen resulting in decreased squeeze film pressure. Also in transverse roughness case high values of magnetic parameter i.e, $M_0 = 3$, couplestress parameter $l^* = 0.3$ and roughness parameter $C = 0.3$ aids in increased squeeze film pressure compared to the nonmagnetic case, Newtonian lubricant case $l^* = 0$ and smooth case respectively compared to longitudinal roughness case.

3.2 Load Carrying Capacity

Figures 5, 6, 7 displays dimensionless load carrying capacity W^* versus amplitude ratio S for different values of C, M_0 and l^*. Load carrying capacity increases in case of transverse roughness for high values of couple stress parameter, magnetic parameter, and roughness parameter and it decreases in longitudinal roughness case. Much higher loads can be sustained by the bearing with transverse roughness but bearing with longitudinal roughness supports the load for a shorter period of time. Also, higher load carrying capacity of the bearing is seen when it is lubricated with couplestress fluids. Porousness effects the load carrying capacity of the bearing, for all values of C, M_0 and l^* the capacity decreases. Because of the porousness fluid escapes from the porous region thus reduces film pressure generation which lowers load carrying capacity. This loss in load capacity is reimbursable if suitable roughness parameter value is chosen.

3.3 Squeeze Film Time

Figures 5, 6, 7 displays dimensionless squeeze film time T^* versus squeeze film height h_0^* for different values of C, M_0 and l^*. The response time of squeeze films is an important factor in designing the bearings. High values of C and M_0 increases the squeeze time and because of the couplestress effects $\left(l^* \to 0\right)$ higher film pressure is seen resulting in higher load capacity consequently response time also increases. This response time shows the elapsed time of the squeeze film to get reduced to some minimum acceptable height for safe function. As compared to the Newtonian lubricant case, the time taken is significantly more for the couplestress fluid lubricant in reducing the film height. Therefore these results show that with the increase in couplestress parameter value response time increases. For all values of C, M_0 and l^* response time increases in case of transverse roughness compared to longitudinal roughness case.

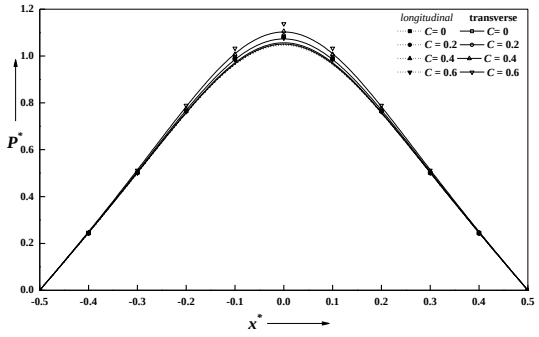

Fig.2. Variation of non-dimensional P^* as a function of x^* for different values of C at $M_0 = 3, l^* = 0.3$ with $y = 0.01$

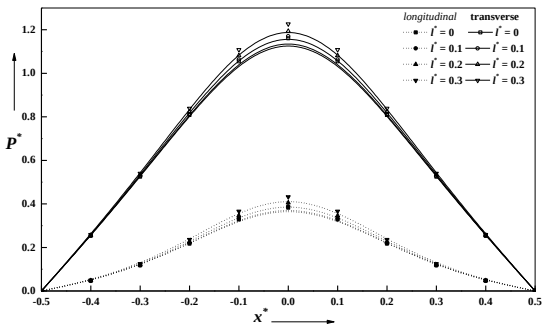

Fig. 3.Variation of non-dimensional P^* as a function of x^* for different values of l^* at $M_0 = 3, C = 0.3$, $y = 0.01$

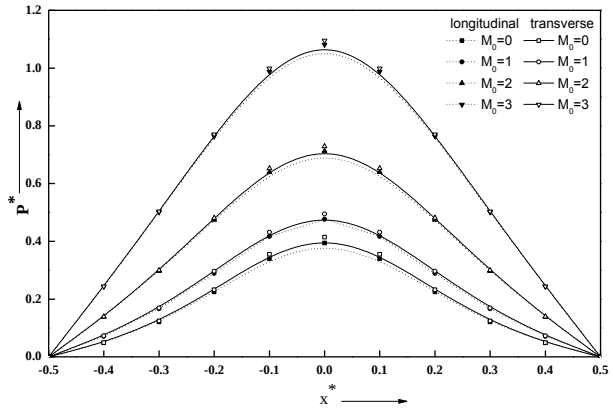

Fig.4 Variation of non-dimensional P^* as a function of x^* for different values of with, and $y = 0.01$

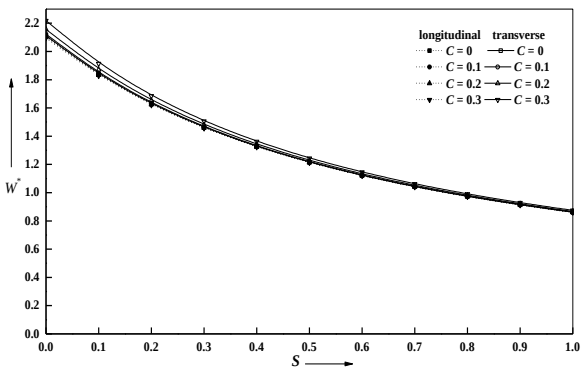

Fig. 5 Variation of non-dimensional W^* with S for different values of C with $M_0 = 3, l^* = 0.3$ and $y = 0.01$

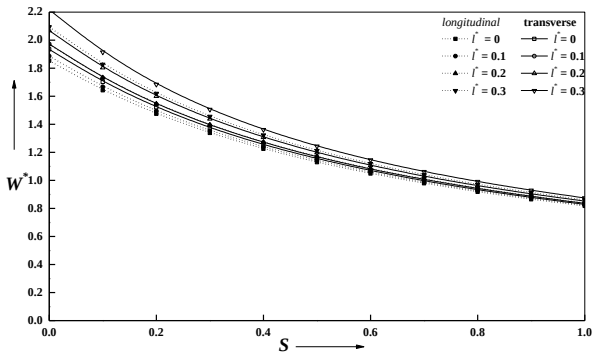

Fig. 6. Variation of non-dimensional P^* with amplitude ratio S for different values of l^* and $M_0 = 3, C = 0.3, y = 0.01$

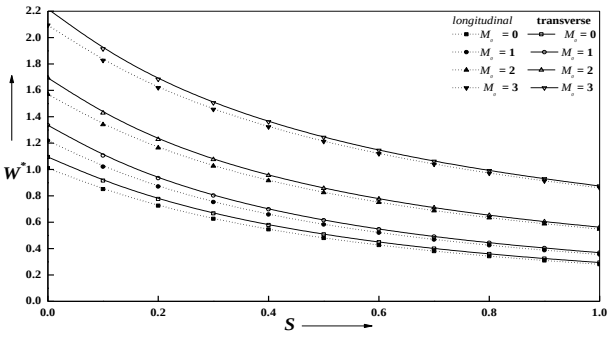

Fig. 7. Variation of non-dimensional W^* with amplitude ratio S for different values of M_0 and $l^* = 0.3, C = 0.3, y = 0.01$

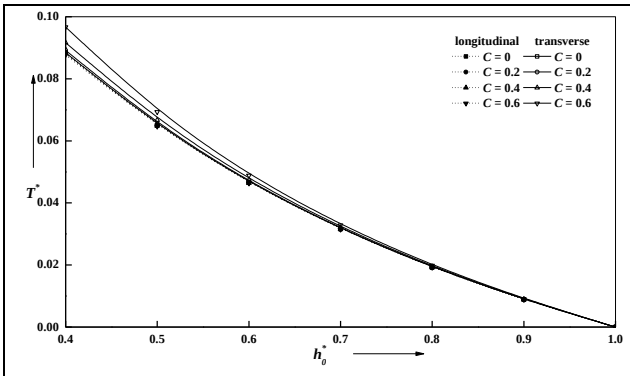

Fig. 8 Variation of non-dimensional T^* with h_0^* for different values of C with $l^* = 0.3$, $M_0 = 3$ and $y = 0.01$.

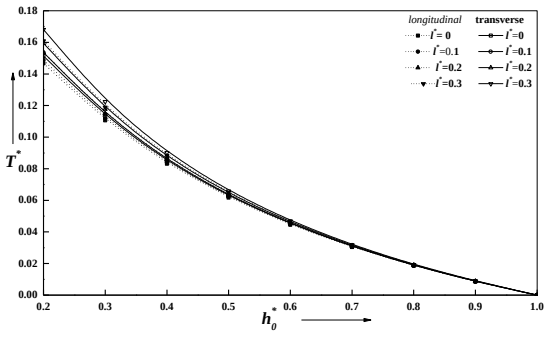

Fig. 9. Variation of non-dimensional T^* with h_0^* for different values of l^* and $M_0 = 3$, $C = 0.3$ at $y = 0.01$.

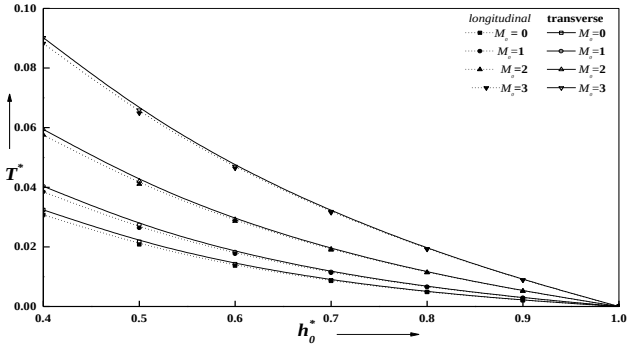

Fig. 10. Variation of non-dimensional T^* with h_0^* for different values of M_0 at $C=0.3$ $l^*=0.3$ and $y=0.01$

Tables

Table 1: Variations for Longitudinal W^*

		$\psi=0$			$\psi=0.01$		
		$C=0$	$C=0.1$	$C=0.2$	$C=0$	$C=0.1$	$C=0.2$
$M_0=0$	$l^*=0$	0.460141	0.459179	0.456317	0.430723	0.429887	0.427399
	$l^*=0.1$	0.471617	0.470604	0.467591	0.437806	0.436942	0.434369
	$l^*=0.2$	0.494997	0.493876	0.490544	0.457682	0.456734	0.453915
	$l^*=0.3$	0.532728	0.531421	0.52754	0.489415	0.488327	0.485093
$M_0=1$	$l^*=0$	0.536233	0.535442	0.533088	0.525157	0.524401	0.522151
	$l^*=0.1$	0.544669	0.543849	0.541405	0.533222	0.532438	0.530105
	$l^*=0.2$	0.568189	0.567281	0.564576	0.555673	0.554808	0.552232
	$l^*=0.3$	0.610201	0.609121	0.605909	0.591398	0.59039	0.587392
$M_0=2$	$l^*=0$	0.762617	0.762131	0.760677	0.757798	0.757319	0.755886
	$l^*=0.1$	0.772191	0.771688	0.770184	0.767244	0.766748	0.765265
	$l^*=0.2$	0.797523	0.79697	0.795315	0.792225	0.79168	0.79005
	$l^*=0.3$	0.83657	0.835925	0.833997	0.830704	0.830069	0.828171
$M_0=3$	$l^*=0$	1.13502	1.13476	1.13398	1.13185	1.13159	1.13082
	$l^*=0.1$	1.14702	1.14675	1.14596	1.14378	1.14351	1.14272
	$l^*=0.2$	1.17621	1.17593	1.1751	1.1728	1.17252	1.17169
	$l^*=0.3$	1.21853	1.21823	1.2173	1.21485	1.21455	1.21362

Table 2: Variations for Transverse W^*

		$\psi=0$			$\psi=0.01$		
		$C=0$	$C=0.1$	$C=0.2$	$C=0$	$C=0.1$	$C=0.2$
$M_0=0$	$l^*=0$	0.460141	0.462054	0.467895	0.430723	0.432214	0.436739
	$l^*=0.1$	0.468304	0.470304	0.476415	0.437806	0.439357	0.444065
	$l^*=0.2$	0.491325	0.493568	0.500434	0.457682	0.459396	0.464605
	$l^*=0.3$	0.528434	0.531072	0.539162	0.489415	0.491384	0.497371
$M_0=1$	$l^*=0$	0.536233	0.5382	0.544208	0.525157	0.526979	0.532532
	$l^*=0.1$	0.544669	0.546724	0.553004	0.533221	0.535122	0.540918
	$l^*=0.2$	0.568189	0.57049	0.577531	0.555673	0.557792	0.56426
	$l^*=0.3$	0.605721	0.608419	0.616692	0.591398	0.593865	0.601409
$M_0=2$	$l^*=0$	0.762617	0.762131	0.760677	0.757798	0.759878	0.766222
	$l^*=0.1$	0.772191	0.771688	0.770184	0.767243	0.769411	0.776029

	$l^* = 0.2$	0.797523	0.79697	0.795315	0.792225	0.794634	0.801999
	$l^* = 0.3$	0.83657	0.835925	0.833997	0.830704	0.8335	0.842065
$M_0 = 3$	$l^* = 0$	1.13502	1.13741	1.14468	1.13185	1.13421	1.14142
	$l^* = 0.1$	1.14702	1.1495	1.15707	1.14378	1.14623	1.15374
	$l^* = 0.2$	1.17621	1.17895	1.18731	1.1728	1.1755	1.18378
	$l^* = 0.3$	1.21853	1.22167	1.23128	1.21485	1.21796	1.22746

Table 3: Variations for Longitudinal T^*

		$\psi = 0$			$\psi = 0.01$		
		$C = 0$	$C = 0.1$	$C = 0.2$	$C = 0$	$C = 0.1$	$C = 0.2$
$M_0 = 0$	$l^* = 0$	0.0199895	0.0199576	0.0198627	0.0190979	0.0190693	0.0189844
	$l^* = 0.1$	0.0202617	0.0202288	0.0201309	0.0193413	0.019312	0.0192246
	$l^* = 0.2$	0.0210301	0.0209943	0.0208877	0.0200263	0.0199945	0.0199001
	$l^* = 0.3$	0.0222679	0.0222271	0.0221058	0.021122	0.0210863	0.0209799
$M_0 = 1$	$l^* = 0$	0.0247445	0.0247197	0.0246457	0.0243877	0.0243638	0.0242925
	$l^* = 0.1$	0.0250297	0.0250041	0.0249277	0.0246628	0.0246381	0.0245646
	$l^* = 0.2$	0.0258238	0.0257958	0.0257124	0.025428	0.0254012	0.0253211
	$l^* = 0.3$	0.0270855	0.0270534	0.0269578	0.0266412	0.0266105	0.026519
$M_0 = 2$	$l^* = 0$	0.0388447	0.0388308	0.038789	0.038668	0.0386542	0.038613
	$l^* = 0.1$	0.039187	0.0391727	0.0391296	0.0390066	0.0389924	0.0389499
	$l^* = 0.2$	0.0400814	0.0400658	0.0400191	0.039891	0.0398756	0.0398295
	$l^* = 0.3$	0.0414368	0.041419	0.0413655	0.0412303	0.0412127	0.0411601
$M_0 = 3$	$l^* = 0$	0.0619329	0.061926	0.0619053	0.0618038	0.0617969	0.0617763
	$l^* = 0.1$	0.0624008	0.0623938	0.0623727	0.0622694	0.0622625	0.0622415
	$l^* = 0.2$	0.0635143	0.063507	0.063485	0.0633774	0.0633702	0.0633483
	$l^* = 0.3$	0.0650789	0.0650711	0.0650475	0.0649341	0.0649263	0.0649028

Table 4: Variations for Transverse T^*

		$\psi = 0$			$\psi = 0.01$		
		$C = 0$	$C = 0.1$	$C = 0.2$	$C = 0$	$C = 0.1$	$C = 0.2$
$M_0 = 0$	$l^* = 0$	0.0199895	0.0200529	0.0202462	0.0190979	0.0191501	0.0193084
	$l^* = 0.1$	0.0202617	0.0203275	0.0205283	0.0193413	0.0193953	0.0195589
	$l^* = 0.2$	0.02103	0.0211027	0.0213245	0.0200263	0.020085	0.0202634
	$l^* = 0.3$	0.0222679	0.0223516	0.0226075	0.021122	0.0211883	0.0213897
$M_0 = 1$	$l^* = 0$	0.0247445	0.0248103	0.0250104	0.0243877	0.0244495	0.0246375
	$l^* = 0.1$	0.0250297	0.0250979	0.0253056	0.0246628	0.0247268	0.0249216
	$l^* = 0.2$	0.0258238	0.0258989	0.0261279	0.025428	0.0254983	0.0257121
	$l^* = 0.3$	0.0270855	0.0271716	0.0274349	0.0266412	0.0267213	0.0269655
$M_0 = 2$	$l^* = 0$	0.0388447	0.0389172	0.0391378	0.038668	0.0387392	0.0389558
	$l^* = 0.1$	0.039187	0.0392621	0.0394907	0.0390066	0.0390803	0.0393046
	$l^* = 0.2$	0.0400814	0.0401635	0.0404137	0.039891	0.0399714	0.0402168
	$l^* = 0.3$	0.0414368	0.04153	0.0418148	0.0412303	0.0413216	0.0416005
$M_0 = 3$	$l^* = 0$	0.0619329	0.0620166	0.0622713	0.0618038	0.0618868	0.0621395
	$l^* = 0.1$	0.0624008	0.0624873	0.0627504	0.0622694	0.0623552	0.0626162
	$l^* = 0.2$	0.0635143	0.0636079	0.0638931	0.0633774	0.0634703	0.0637532
	$l^* = 0.3$	0.0650789	0.0651838	0.0655038	0.0649341	0.065038	0.0653553

4. CONCLUSION

Based on the stochastic model of Christensen, the effects of surface roughness and porousness on the magnetohydrodynamic squeeze film lubrication of cosine form of convex curved plates with couplestress effects are presented. To account for the presence of roughness the modified form of stochastic Reynolds equation leading the film pressure is obtained.

i) As the roughness parameter value approaches zero, the results reduce to the smooth surface case. According to the derived results, the roughness pattern and height of roughness imply an influence on the squeeze film characteristic of the convex curved plates.

ii) An enhancement in the load carrying capacity and lengthened response time is noticed in presence of couplestress fluid lubricant compared to the Newtonian lubricant case. For high values of l^* the quantitative effects of couplestresses are more prominent therefore it implies improved squeeze film characteristic of the system.

iii) Increase in permeability decreases pressure distribution, load capacity and response time compared to the classical case. In general squeeze film, characteristics can be increased by giving suitable values to the magnetic parameter, roughness, and couplestress parameter and hence bearing function can be improved.

5. REFERENCES

[1]. Hays DF. Squeeze Films for Rectangular Plates. *J Basic Eng-T ASME* 1963; 85:243-246.
[2]. Murti PRK... Squeeze Films in Curved Circular Plates. *J Lubric Tech-T ASME* 1975; 97: 650-652.
[3]. Pinkus O and Sternlicht B. Theory of Hydrodynamic Lubrication. NewYork: McGraw Hill, 1961.
[4]. Lin JR. Pure Squeeze Film Behavior in a Hemispherical Porous Bearing Using the Brinkman Model. *STLE Tribol T* 1996; 39: 769-778.
[5]. Hammock BJ. Fundamentals of Fluid Film Lubrication. New York: McGraw-Hill, 1994.
[6]. Lin JR, Liao WH, and Hung CR. The Effects of Couple Stresses in the Squeeze Film Characteristics Between a Cylinder and a Plane Surface. *J Mar Sci Technol* 2004; 12:119-123.
[7]. Lin JR. Squeeze Film Characteristics between a Sphere and a Flat Plate: Couple Stress Fluid Model. *Comput Struct* 2000; 75:73-80.
[8]. Barus C. Isothermals, Isopiestics, and Isometrics Relative to Viscosity. *Am. J. Sci.*1893; 45:87-96.
[9]. Lu RF and Lin JR. A Theoretical Study of Combined Effects of Non Newtonian Rheology and Viscosity-Pressure Dependence in the Sphere-plate Squeeze-film system. *Tribol Int* 2007; 40:125-131.
[10]. Christensen H. Stochastic models for hydrodynamic lubrication of rough surfaces. *Proc. Inst.Mech. Eng.* 1969; 184:1022–1033.
[11]. Bujurke NM and Kudenatti RB. MHD lubrication flow between rough rectangular plates. *Fluid Dyn Res* 2007; 39(4):334–345.
[12]. Naduvinamani NB, Fatima ST and Jamal S. Effect of roughness on hydromagnetic squeeze films between Porous rectangular plates. *Tribol Int* 2010; 43(11):2145–2151.
[13]. Bujurke NM and Naduvinamani NB. A note on squeeze film between rough anisotropic porous Rectangular plates. *Wear* 1998; 217(2):225–230.
[14]. Naduvinamani NB and Rajashekar M. Effect of surface roughness on magneto-hydrodynamic Squeeze film characteristics between a sphere and a porous plane surface. *Ind Lubr Tribol* 2012; 66(3): 365 – 372.
[15]. Naduvinamani NB, Fathima ST, and Hanumagouda BN. Magneto-hydrodynamic couple stress squeeze film Lubrication of circular stepped plates. *Journal of Engineering Tribology* 2011:225(I):111–119.
[16]. Stokes VK. Couple stresses in fluids. *Phys. Fluids*, 1966: 9:1709–1715.
[17]. Syeda Tasneem Fathima, Naduvinamani NB, Shivakumar HM and Hanumagowda BN. A study on the Performance of hydromagnetic squeeze film between anisotropic porous rectangular plates with couplestress Fluids. *Tribology Online* 2014: 9:1– 9.

NOTATION

B_0 Applied magnetic field in the $z-$direction
c Maximum asperity deviation from the nominal film height
C Dimensionless roughness parameter (c/h_0)
H Film thickness
L Length of the plates
d Amplitude of the cosine function
b Width of the curved plates
A Dimensionless amplitude ratio of the cosine function
h_0 Minimum film thickness
h_0^* Dimensionless film thickness after time Δt
h_s Stochastic film thickness

k Permeability of the porous matrix
p Hydrodynamic film pressure
p^* Pressure in the porous region
M_0 Magnetic Parameter $\left(= B_0 h_0 (\frac{\sigma}{\mu})^{1/2} \right)$
u, w Velocity components in film region
u^*, w^* Velocity components in porous region
x, y, z Local Cartesian co-ordinates
m Porosity
P^* Dimensionless pressure $\left(= \frac{p h_0^3}{\mu L^2 (-dH/dt)} \right)$
t Mean time of approach
l Couplestress fluids $\left(\eta / \mu \right)^{1/2}$
l^* Dimensionless parameter $\left(2l / h_0 \right)$
T^* Dimensionless time of approach $\left(= \frac{h_0^2 W t}{\mu L^3 b} \right)$
V Squeezing Velocity $\left(-\frac{dH}{dt} \right)$
W^* Dimensionless load carrying capacity $\left(= \frac{h_0^3 W}{\mu L^3 b(-dH/dt)} \right)$

GREEK SYMBOLS

σ Conductivity of fluid
μ Lubricant viscosity
ξ Random variable
$\overline{\sigma}$ Standard deviation
ψ Nondimensional permeability parameter
δ Porous layer thickness
δ^* Nondimensional porous layer thickness

